Helium Neon Laser: Analysis of different Resonator Configurations and Application in Laser Interferometry.

Renu Raman Sahu

October 3, 2018

Abstract

Light amplification by stimulated emission of radiation, acronymed LASER, finds itself not only in a wide range of applications but is also of much theoretical and experimental interest. In this experiment, the properties of a particular laser system, viz. Helium-Neon laser was analyzed. After careful analysis, a suitable configuration was chosen to obtain a beam of sufficient intensity and suitable radius so as to illuminate a miniature spring for solving its structure.

In the first part of the experiment, the wavelength of the Helium-Neon laser was determined to be $\lambda = 619.31 \pm 14.58$. The analysis of different resonator configurations was undertaken to study the beam shape and power output of the beam. The quality of the beam was analyzed, M^2 was found to be 0.751 ± 0.054.

Having studied various laser parameters, HR flat/flat HR flat/1000mm resonator configuration was chosen with a resonator length of 450 mm, for laser interferometry in order to solve the structure of a spring. A left-handed spring was made manually, and it's diameter(a) and pitch(p) were determined by using principles of interference and diffraction to be $a = (9.63 \pm 0.13) \times 10^{-2}$ mm and $p = 0.066 \pm 0.002$ cm. The pitch was also determined using a traveling microscope and was found to be $p = 0.066 \pm 0.007$ cm, which is in excellent agreement.

Also, a brief discussion of further experimental work, which can be performed using apparatus, is presented.

Contents

1 Introduction

As implied by the name, in a laser, light waves are amplified by stimulated emission. Two different kinds of emission processes, viz. spontaneous and stimulated, were first predicted by Einstein in 1917. Utilization of stimulated emission for construction of coherent light sources was proposed and in 1960, Maiman demonstrated the first working laser. Since then, rapid development in the field has taken place and different lasing systems have been studied.

A laser has three main components, namely, the amplifying medium, the pump, and the optical resonator. The amplifying medium is a collection of atoms, molecules or ions which act as an amplifier for the light waves. Generally, the constituents of the amplifying medium are in the ground state. Hence if a wave passes through the medium, then the number of absorptions exceed the number of emissions and this results in attenuation of the passing light wave. So in order to have amplification, it is necessary to have a state of the system in which most of the constituents molecules are in higher energy state as compared to that in lower energy states. This state is known as population inverted state. Now if a light wave passes through a population inverted medium the number of emissions will be more than the number of absorptions and hence light will be amplified. In order to maintain a continuous beam of light, the medium should be maintained at population inverted state. This is the job of a pump which provides energy to the system so as to remain in this state [1].

The optical resonator consists of a pair of mirrors facing each other. It provides optical feedback to the to the amplifier so that it can act as a source of radiation. The resonators can support only certain specific field configurations and certain specific oscillation frequencies. Hence for a given resonator configuration, the shape of the laser beam is fixed. It varies as we change the resonator. A laser beam is characterized by parameters of a Gaussian beam. In this experiment, we shall study the beam shape and output power for different resonator configurations.

2 Helium-Neon Laser system

In order to study laser properties, we use the Helium-Neon laser system. It is the first continuous laser. The first HeNe laser invented by Javan et. al. in 1961 oscillated at a frequency of $1.5\mu m$. The first red laser at 632.8 nm was constructed a year later by White and Ridgen.

Owing to several careful spectroscopic investigations the energy level of inert gases and their atomic structure was well understood. Using this knowledge, Schawlow and Towne gave a criterion which showed that in Helium-Neon system population inversion was possible. The lifetime of s-states and p-states was well known. It was well established that the lifetime of s-states was ten times larger than p-states. Hence population inversion can be achieved if there is an s-state with higher energy than p-state. The energy level diagram of Helium-Neon system is shown in the following figure.

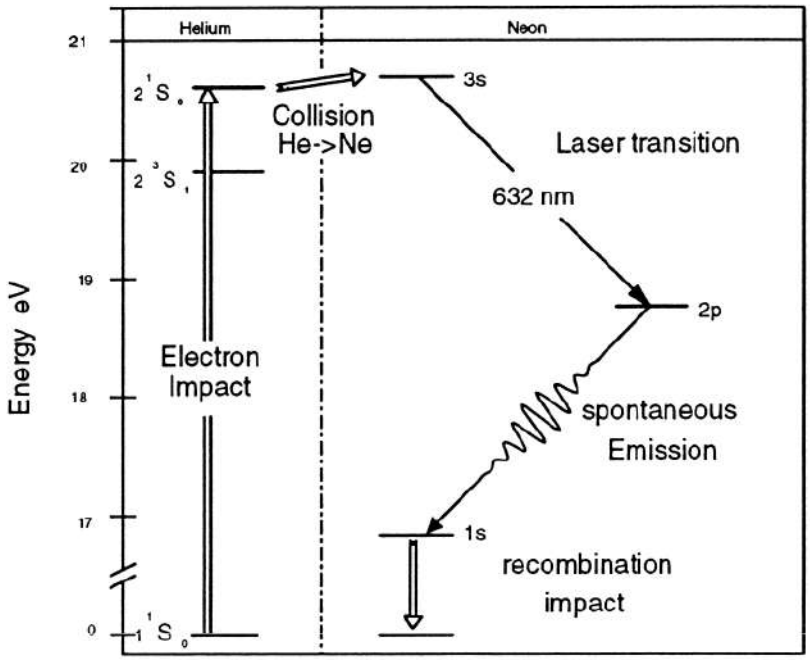

The above figure shows only the energy levels relevant for a discussion of the red laser beam at 632 nm. The left side of the figure shows the low levels of Helium. A characteristic of helium is that its excited states with the lowest energy are metastable, i.e., optical transitions to the ground state $1S_0$ are not allowed because selection rules forbid it. These excited states are populated by electron collisions in a gas discharge. This is an example of the collision of second type. A collision is said to be of second type if the internal energy of the colliding particles changed in the reaction.

Besides electron collisions there are also atomic collisions of second type in which an excited helium atom state decays without photon emission transferring its energy to a neon atom. Through both these processes, the Neon system gets population inverted.

Inspection of the energy level diagram shown above reveals that $2S_0$ level of helium is slightly below the $3S$ level of Neon. But this small gap is overcome by the thermal energy k_BT. Since the lifetime of s-state is about ten times more than that of a p-state, an immediate population inversion between 3s and 2p states is generated. The 2s level is emptied due to spontaneous emission to 1s levels. This particular state is decayed into the ground state through wall collisions since optical transitions are not allowed. This requires the capillary wall to be kept as small as possible. On the other hand more the active volume, more is the output power. So there is a trade-off and an optimum volume has to be chosen.

The 3s states are populated by Helium atoms of $2S_1$ states, in the process of atomic collision with the Neon atoms. Out of four $3S$ substates, the $3S_2$ state is

the most populated due to the collision. Visible transitions take place between $3S_2$ to $2Pstates$ [2].

3 Experimental Apparatus

3.1 Optical Bench and Conventions used

The components of the apparatus were mounted on an optical bench. A scale of least count 1 mm was there on it to mark the positions of the components. Viewing perpendicular to the scale on optical bench, to it's left, an alignment laser with a diaphragm in front of it was mounted. Also a there was a diaphragm on the right. There are holes at the center of the diaphragm. This setup was used for alignment. Henceforth in the report whenever we shall refer to "left" or "right", it is with respect to this particular configuration. The axis along the optical bench will be referred to as z-axis.

Mirrors were used for resonators. Only plane mirrors and concave mirrors were used in this experiment. The notation for a plane mirror is "HR flat/flat". Here HR stands for High Reflecting. The notation for a concave mirror of certain radius of curvature, say 1000 mm, is "HR flat/1000". Suppose a resonator configuration is such that on left there is a plane mirror and on right there is a concave mirror of radius of curvature 1000mm, then the configuration will be denoted as "HR flat/flat HR flat/1000 mm". It is understood that the reflecting side of the left mirror is towards the right and the concave reflecting surface of the right mirror is towards left.

3.2 Laser tube characteristics and Polarization of light

Polarisation also characterizes photons. In general, the isotropic sensitivity of gas atoms in the gas discharge towards all polarisations is expected. Also in a small volume element, the velocity distribution of atoms is also spatially isotropic. But since the geometry of the discharge tube is such that it is elongated in z-direction. Hence it is in this direction that the gain is enhanced.

Since the gas discharge has a very low density, the optical gain is quite low. So reflection on the laser tube's confinement has to be avoided. To achieve this, optical windows at Brewster angle are used. This results in zero reflection for a particular polarization. On the other hand, other polarisations are lost due to reflection. Hence the laser tube's gain depends on polarisation, and a HeNe laser beam with Brewsters window is fully linearly polarized. The following figure is of the discharge tube. Note that the ends of discharge tube are at a certain angle, which is brewsters angle. The illuminated part in the tube is the capillary containing helium Neon mixture.

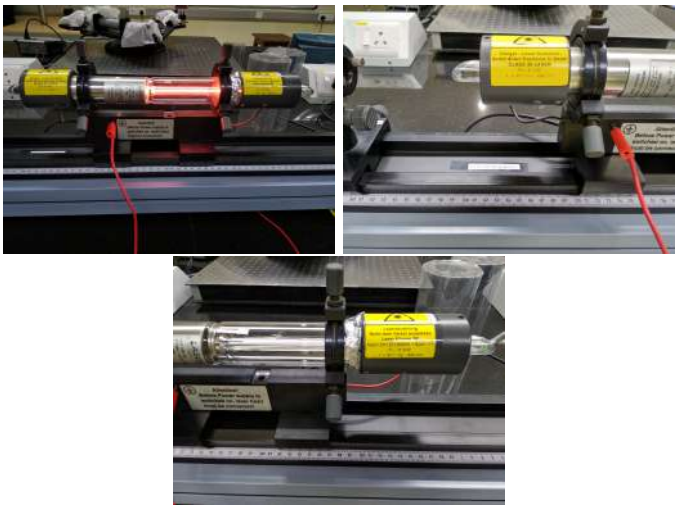

3.3 Resonators

As discussed earlier, in order for the amplifier to be an oscillator (source of radiation) it is important to give optical feedback. Usually, the optical cavity for a HeNe laser is a Fabry-Perot resonator, consisting of two opposite mirrors with laser tube in between. The transmission of a Fabry-Perot resonator is a frequency comb with spikes that are equidistant in frequencies, and are the harmonics of the first natural frequency. Since the gain of the laser tube is low, reflections losses are unaffordable and hence the mirrors should have high reflectivity to make spontaneous possible. Spontaneous oscillation is also referred to as laser ignition or lasing condition.

We performed the experiment with plane mirrors (HR flat/flat) and two concave mirrors of radii of curvature 1000 mm (HR flat/1000 mm) and 1400 mm (HR flat/1400 mm). We studied three different resonator configurations, viz., HR flat/flat HR flat/1000 mm, HR flat/flat HR flat/1400 mm and HR flat/1000 mm HR flat/1400 mm.

4 Helium-Neon laser system: Experiment and Analysis

We now discuss the experimental steps we have taken and the results we have obtained for the corresponding experimental study. Once we chose a resonator configuration, the first task was to obtain a stable lasing condition. First of all, we determined the wavelength of Helium-Neon laser and that of alignment laser. Then resonator configurations were changed and beam shape analysis was performed. Also, the power dependence was studied for each resonator.

4.1 Obtaining Lasing condition

A green alignment laser with a diaphragm was provided to align the optical bench. Another diaphragm was on the right. The circular diffraction pattern of the green laser with the central maximum on the hole of the right diaphragm was visible. A flat mirror and a concave mirror (1000 mm focal length) was mounted and was adjusted so that the diffraction pattern of the alignment laser on the right diaphragm was visible. This ensured that the mirrors reflected the point of incidence on the other mirror. Then the laser tube was placed and was switched on. The tube was adjusted so that the green laser was not get reflected by the laser tube. Playing around with the knobs for some time resulted in lasing.

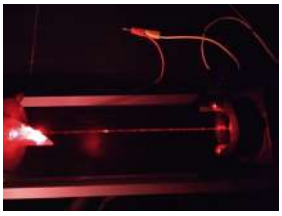

The fine red line visible in above figure is the Helium-Neon laser beam. The red illuminated region in the left is Brewsters window. On the right is the resonator mirror.

4.2 Wavelength Determination

The wavelength of the alignment laser and that of Helium-Neon laser was determined. We briefly discuss the principle of the experimental method used to do so.

4.2.1 Working Formula and Analysis

The wavelength of monochromatic laser light can be determined by the angle of diffraction for different order peaks. The formula for wavelength give the order and corresponding diffraction angle ($\tan^{-1}\alpha$) is

$$\lambda = \frac{l}{n} \sin\tan^{-1}(\alpha) \tag{1}$$

where α is the slope of d_n vs. D plot. Here D is the distance between the diffraction grating and vertical scale, while d_n is that of the central maxima and the n^{th} order diffraction peak. Here l is the slit width of diffraction grating. Since we are given a grating of 600 lines per mm,

$$l = (1/0.6) \times 10^{-6} = 1.667\mu m$$

The slope of a linear plot of d_n vs. D, where both of them are in same units, gives α. The following plots depict the distance of the first and second order

peak (d_1 and d_2 respectively) from the central maxima for different ditances, D, between the diffraction grating and the vertical scale.

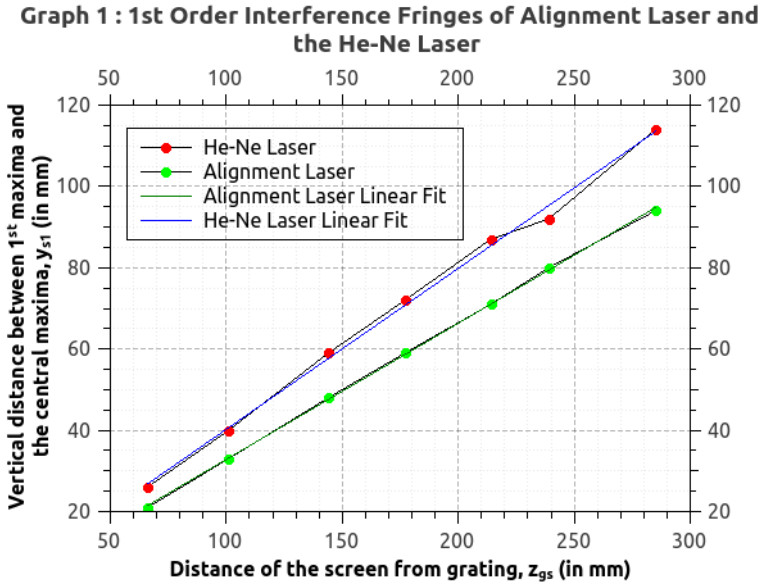

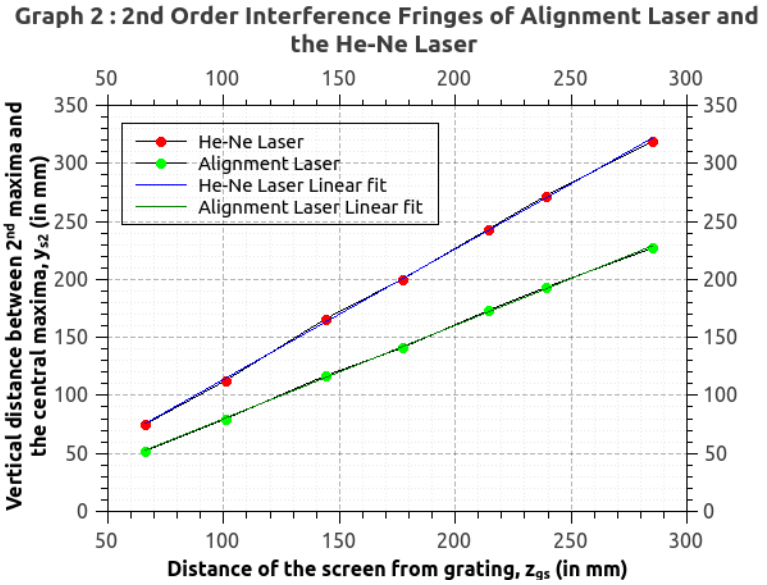

4.2.2 For Alignment laser

Following table is the data for the wavelength measurement of alignment laser.

D (cm)	d_1(mm)	d_2(mm)
14.4	48	117
6.6	21	52
28.5	94	227
23.9	80	193
21.4	71	173
17.7	59	141
10.1	33	80

Distance between diffraction grating and vertical scale (D in cm), distance of first and second order maxima from the central maximum (d_1, d_2 in mm respectively) are tabulated above.

The wavelength of alignment laser is obtained from the slope of the plot d_n vs. D.

The linear fit has following slope $\alpha_{g1} = (0.3349 \pm 0.0029)$ and $\alpha_{g2} = (0.8046 \pm 0.0078)$. With this slope the wavelength (using eqn. 1) of alignment laser is

$$\lambda_{g1} = (530.36 \pm 4.19)\text{nm}$$

$$\lambda_{g2} = (523.43 \pm 6.14)\text{nm}$$

We take the wavelength of alignment light to be the average and propagate the error so as to obtain

$$\lambda_g = 526.892 \pm 7.44\text{nm}$$

4.2.3 For Helium-Neon laser

Following table is the data for wavelength measurement of Helium-Neon laser.

D (cm)	d_1(mm)	d_2(mm)
14.4	59	166
6.6	26	75
28.5	114	319
23.9	92	272
21.4	87	243
17.7	72	200
10.1	40	113

The distance between diffraction grating and vertical scale (D in cm), distance of first and second order maxima from the central maximum (d_1, d_2 in mm respectively) are tabulated above.

The wavelength of alignment laser is obtained from the slope of the plot d_n vs. D.

The linear fit has following slope $\alpha_{r1} = (0.396 \pm 0.010)$ and $\alpha_{r2} = (1.124 \pm 0.012)$. With this slope the wavelength (using eqn. 1) of HeNe laser is

$$\lambda_{r1} = (614.88 \pm 13.43)\text{nm}$$
$$\lambda_{r2} = (623.75 \pm 5.68)\text{nm}$$

We take the wavelength of alignment laser to be the average and propagate the error so as to obtain

$$\lambda_r = 619.31 \pm 14.58\text{nm}$$

4.3 Beam Diameter Analysis

In this analysis we plot and compare the calculated and experimentally observed plots of beam-waist radius w_0 and beam radius at the concave mirror w_d as the mirror distance varies. The beam radius at $1400mm$ at the end of the optical bench has been determined for a given d. We thus determine how the beam shape changes as the resonator size increases. Here, we used HR flat and HR flat/1000 mm concave mirrors in the resonator.

4.3.1 The experimental setup and Gaussian beam

The experimental setup consisted of two mirrors as resonators. HR (high reflecting) mirror was on the leftmost part of the optical bench with its high reflecting surface facing rightwards. The right mirror was an HR flat/1000 mm mirror, with its concave part facing leftwards. This clearly implies that the beam waist (parallel part of Gaussian beam) is near the left mirror. The curvature of the Gaussian beam on the right one matches with the latter. So the radius of curvature of the left and right mirror is

$$r_1 = \infty$$

and

$$r_2 = 1000 \text{ mm}$$

The wavelength of Helium-Neon laser is determined to be

$$\lambda_r = 619.3114.58 \text{ nm}$$

The distance between the two mirrors d is known.

4.3.2 Formulae for $w_0(d)$ and $w_d(d)$.

Suppose the beam waist is at the origin and has a radius w_0. The beam width of a Gaussian beam increases as

$$w(z) = w_0\sqrt{1 + \left(\frac{z}{z_0}\right)^2} \tag{2}$$

where

$$z_0 = \frac{\pi w_0^2}{\lambda}$$

is known as Rayleigh range or depth of focus.

The wavefronts in a Gaussian beam have a curvature

$$R(z) = z\left(1 + (z_0/z)^2\right) \tag{3}$$

Far from the beam waist ($z > |z_0|$) a Gaussian beam opens like a cone of angle 2α where

$$\alpha = \tan^{-1}(w(z)/z) \approx w(z)/z \tag{4}$$

From the formula of rayleigh range w_0/z_0 is determined to be $\lambda/\pi w_0$. So the angle

$$\alpha = \tan^{-1}(w_0/z_0) \approx w_0/z_0 = \lambda/\pi w_0$$

For the system we are considering, radius of curvature at $z = d$ is

$$R(d) = r_2 = d\left(1 + \frac{z_0^2}{d^2}\right)$$

Rearranging the above expression to obtain z_0, we get

$$z_0 = \sqrt{d(r_2 - d)}$$

with the distance between mirrors being less than radius of curvature of the concave mirror ($d < r_2$). Now substituting the expression for Rayleigh range in above we obtain the expression of w_0 in terms of d, r_2 and λ.

$$w_0 = \sqrt{\frac{\lambda}{\pi}\sqrt{d(r_2 - d)}} \tag{5}$$

The equation for the beam radius at the right mirror obtained using equation 2 is

$$w(d) = \sqrt{\frac{\lambda}{\pi}\sqrt{d(r_2 - d)} + \sqrt{\frac{d^3}{r_2 - d}}} \tag{6}$$

The angle of divergence is obtained using eqn. 4

$$\alpha = \sqrt{\frac{\lambda}{\pi}\frac{1}{\sqrt{d(r_2 - d)}}} \tag{7}$$

4.3.3 Analysis and Results

The following plot gives depicts the experimentally obtained values of w_0 and w_d against d. The data points match well with the calculated plot. Following table shows the experimentally obtained data for w_0 and w_d for different d.

Sl. No.	d (in mm)	w_0	w_d
1	450	0.35	0.475
2	500	0.35	0.525
3	550	0.35	0.575
4	600	0.375	0.6
5	650	0.375	0.625
6	700	0.375	0.65
7	750	0.35	0.65
8	800	0.325	0.7
9	850	0.275	0.775
10	900	0.225	0.875

Graph 3 : The beam radius of right mirror (w_d, in mm) and beam waist radius (w_0, in mm)

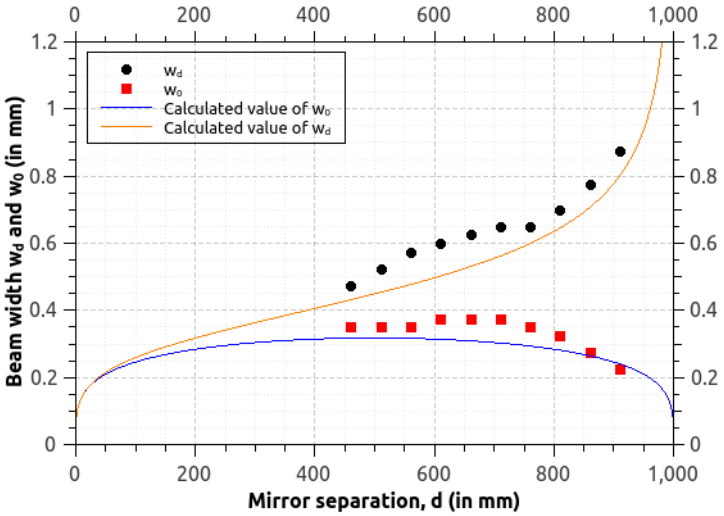

The plot for w_0 and w_d are given according to the expression of eqn. 7. This reveals that the Helium-Neon laser beam has characteristics of a Gaussian beam for the chosen resonator configuration.

4.3.4 Beam radius at 1400 mm from beam waist.

At 1400 mm from the beam-waist we measure the laser power on a small cross section (dimension 0.3mm$\times$ 0.3mm) of a detector along the diameter of bright spot on right diaphragm. The intensity profile was Gaussian, as evident from the following plot.

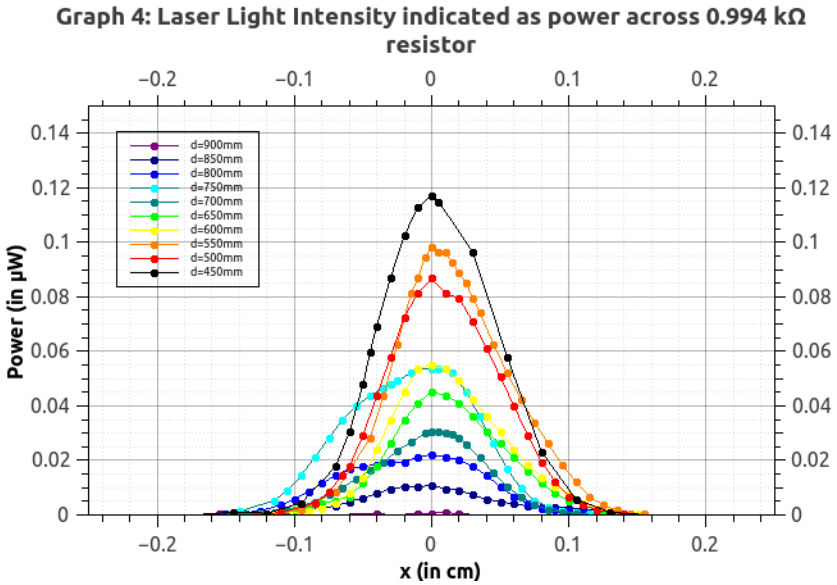

The data points fit nnicely with Gaussian curve. Standard deviation (σ) were determined for each of them and was multiplied with $\sqrt{2}$ to obtain beam radius at 1400 mm (w_{1400}) for each mirror separation d. Using the values of w_0 and wavelength of HeNe Laser λ_r, we obtain M^2 values using the formula

$$M^2 = \pi \alpha w_0 / \lambda \tag{8}$$

The following table shows angle measurement results and the plot shows the divergence angle α for different mirror distances, d.

Sl. No.	d (in mm)	σ (in mm)	w_{1400} (in mm)	α (in rad)
1	450	0.41078	0.5809	0.000414950438435
2	500	0.408365	0.5775	0.000412510920458
3	550	0.405565	0.5736	0.000409682493811
4	600	0.38819	0.5490	0.000392131096171
5	650	0.395715	0.5596	0.000399732492877
6	700	0.400615	0.5666	0.000404682239544
7	750	0.495325	0.7005	0.000500353767375
8	800	0.52232	0.7387	0.00052762282811
9	850	0.53503	0.7566	0.000540461863289
10	900	0.461585	0.6528	0.000466271228487

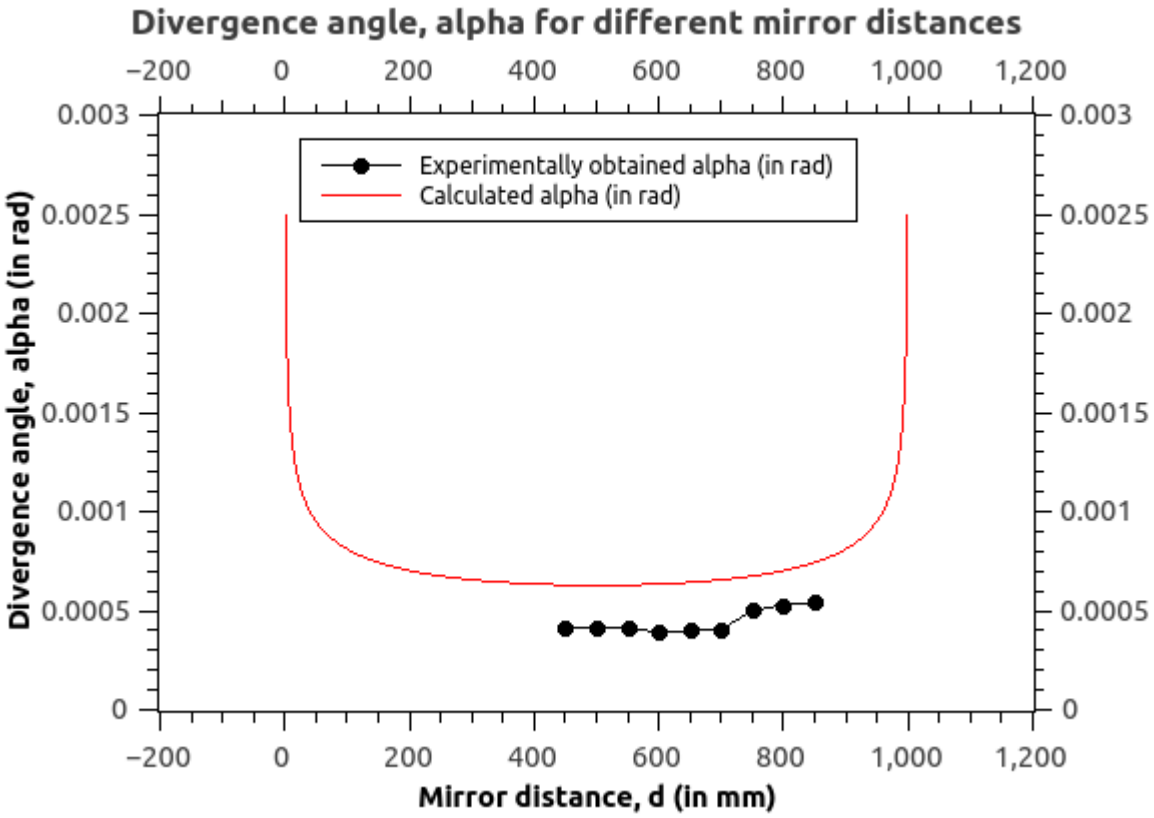

The calulated and the experimentally obtained values of α are offset almost by a constant.

4.3.5 Determination of M^2

The quality of the beam is described by comparing it with a Gaussian beam. It is quantified by Beam Parameter Product (BPP), which is defined as

$$BPP = \alpha.w_0$$

Note that BPP has dimensions of length. So it is customary to divide it with a reference quantity with dimensions of length. A natural choice is scalar multiple wavelengths of the beam. BPP divided by λ/π is according to ISO 11146, a measure of beam quality and called M^2. Thus we obtain eqn. 8.

The table for determination M^2 is given below.

d (in mm)	σ (in mm)	α (in rad)	w_0	M^2	Error in M^2
450	0.411	0.0004150	0.35	0.737	0.118
500	0.408	0.0004125	0.35	0.732	0.123
550	0.406	0.0004097	0.35	0.727	0.151
600	0.388	0.0003921	0.375	0.746	0.150
650	0.396	0.0003997	0.375	0.760	0.135
700	0.401	0.0004047	0.375	0.770	0.124
750	0.495	0.0005004	0.35	0.888	0.166
800	0.522	0.0005276	0.325	0.870	0.174
850	0.535	0.0005405	0.275	0.754	0.185
900	0.462	0.0004663	0.225	0.532	0.194

We obtained M^2 values less than unity, with a mean value of 0.751 and 0.054 as the root mean square of error. For the best quality beams $M^2 = 1$. The M^2 value being less than unity implies that the beam we obtained is not exactly Gaussian.

4.4 Output power dependence

We studied the output power dependence on the resonator length, cavity position and on discharge current.

4.4.1 Output Power dependence on Resonator length.

In this experiment, the laser tube and HR flat/flat on left of the resonator was kept fixed. The resonator length was increased by moving the concave mirror on the right away from the laser tube. The following plot depicts the power output in $\mu Watt$ for two different mirror configurations viz. HR flat/flat, HR flat/1000mm and HR flat/flat, HR flat/1400mm.

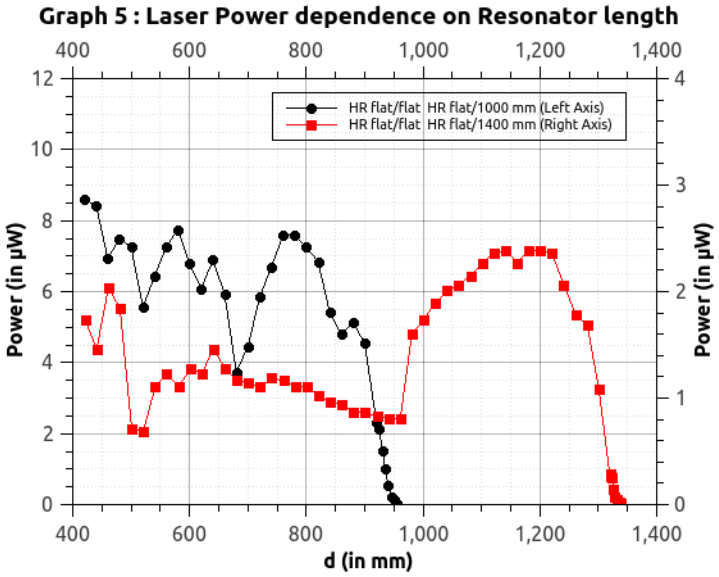

The power output non-zero with some irregularities for a significant length and drops drastically as resonator length reaches the focal length of the concave mirror. Since the power output of 1400mm concave mirror configuration has less power output than that of 1000mm, we conclude that for a hemispherical resonator configuration of larger radius of curvature has low power output.

4.4.2 Output power dependence on cavity position.

This experiment was done for two resonator configurations. The first resonator was HR flat/flat and HR flat/1000 mm mirror configuration. Right edge position of left clamp of laser tube was noted for the tube tube positions. This experiment was done for two different resonator length viz. $d = 700mm$ and $d = 850mm$. The plot of output power for different cavity position is given below.

Graph 6: Laser Power in dependence to Laser Tube Position

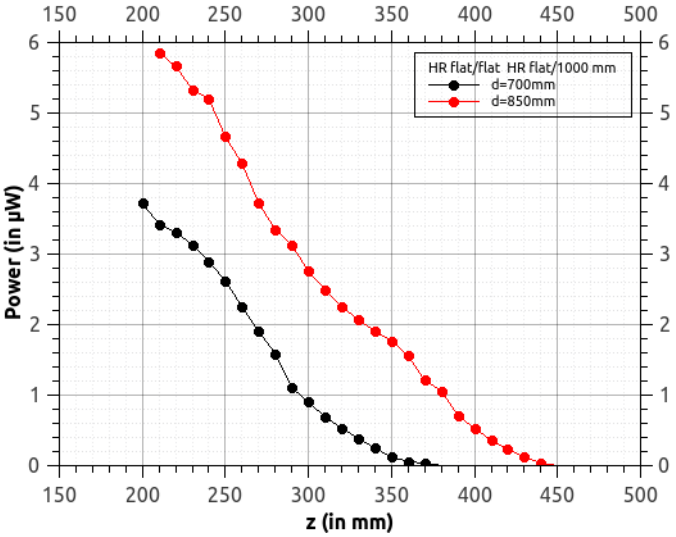

We observe that as the laser tube approaches the concave mirror the output power starts decreasing. Nearer the tube is to the flat mirror, more is the output power. We also observe that for larger resonator length, the output power is more.

The following plot is for HR flat/flat, HR flat/1400 mm resonator configuration. Here also, power decreases as the tube moves towards the concave mirror.

Graph 7: Laser power dependence on Laser Tube positions mirror spacing, d=1050mm

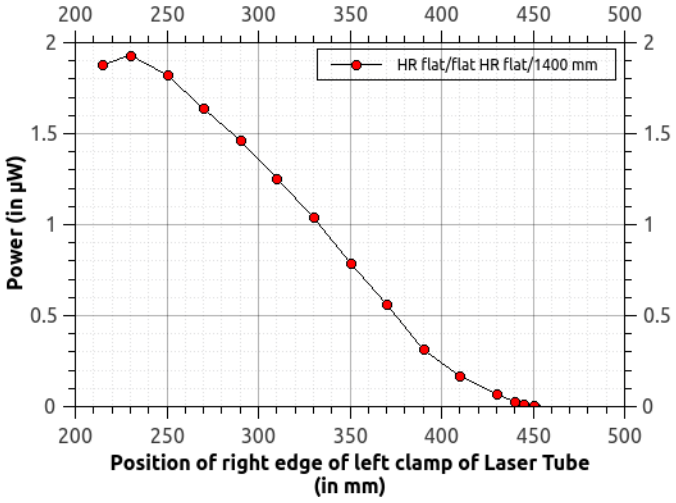

4.4.3 Output power dependence on Discharge current.

This experiment was performed for resonator configuration HR flat/flat, HR flat/1400 mm. The resonator length was fixed to be $d = 450mm$ and the laser tube was also fixed. The discharge current was varied on the power supplier from 4 mA to 9 mA. The power output is shown in the following plot against the discharge current.

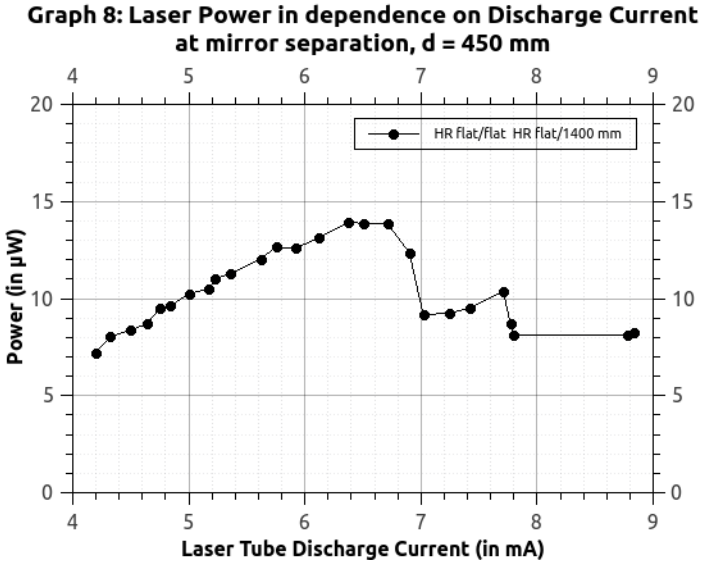

The output power is almost the varies from $6\mu Watt$ to $14\mu Watt$. The peak value of power is attained at around $6.5mA$.

5 Choosing the laser configuration

In the previous part of the experiment, we have determined various parameters for laser configurations. To study the miniature spring we require large power and small beam radius.

The beam waist analysis reveals that the laser beam coming out of the flat mirror in the hemispherical configuration should be used with $d \approx 800mm$. On the other hand, power maximization requires $d = 450mm$. The latter configuration is easier for analysis. We choose HR flat/ flat HR flat/1000mm resonator configuration as the power output was more in this setup as compared to other configurations we tried.

6 Application of Helium-Neon laser to solve the structure of Spring.

A spring, in general, is a helical structure with a certain spring constant that depends upon the material it is made up of. We are particularly interested in its structure, and not it's material properties. One encounters springs of different sizes in many different fields of application and of academic interest. We are concerned with those of sizes of order $10^{-6}m$ to $10^{-9}m$. Since the wavelength of visible light is comparable to these orders of magnitude, it can be used to probe the structure of springs of these sizes.

We briefly describe how we made the spring. In the following two sections we describe the basic equations of diffraction and interference and how the former can be used to determine the diameter of a wire (as we would be using wire to make springs), and the latter can be used to determine the slit width in a double slit experiment. In the section following we shall show how we can apply these to solve the structure of a spring. By solving the structure of a spring we mean determination of its pitch and helicity. As of now, we believe that it is feasible to determine the pitch using the given apparatus.

6.1 Making of Spring

To obtain diffraction and interference pattern with large fringe widths, we need to make a very small spring. In fact, we intend to develop this method to solve structures of small springs.

We have made the spring using a thin copper wire from a cable. With the help of a tweezer, the copper wire was held tight to the base wire. The base wire is a cylindrical metallic body over which we wrap the material of the spring. We used circuit wire as a base to our sprong. Then carefully wrapping of the copper wire around it was done. It was ensured that there is no gap between the two strands of wire on the base. In the process, we obtain a right circular cylinder. The with the help of tweezer it is pushed to the end of base wire. Another tweezer was used to pull the free end of the spring. Following is the picture of the wire strand we used for making the spring.

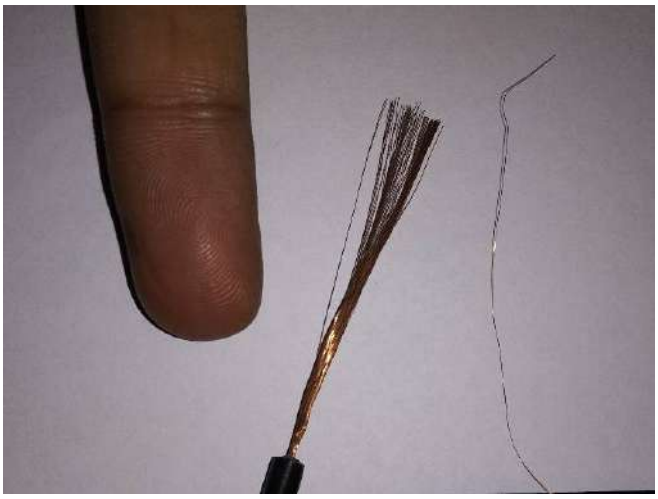

The spring we made is shown in the following picture. For the sake of comparison, we have put the top part of index finger in the picture.

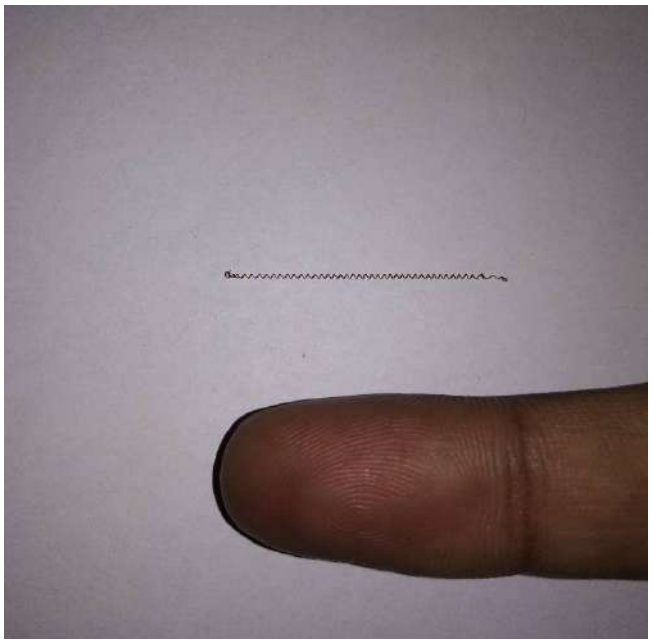

We determined the pitch of the spring using a traveling microscope with least count $0.001cm$. Using this instrument the pitch was determined to be 0.066 ± 0.007 cm.

6.2 Diffraction and determination of the width of a wire

Suppose a thin wire of diameter a is illuminated with a monochromatic beam and a screen is placed D distance away from the wire on the opposite direction of the incident light. Dark and bright fringes are obtained as a result of diffraction. A phase difference of an integral multiple of 2π between superimposing waves will result in constructive interference and hence bright fringes. At an angle θ with the incident beam, a dark fringe is obtained on the screen placed D distance away if

$$a \sin\theta = n\lambda$$

where n is a natural number [3]. In this article, we are concerned with the experimental technique used for our purpose.

Given the wavelength of light, the experimentally accessible quantity is θ. The ratio of the distance between the central maxima and n^{th} order bright fringe to that of the screen and wire gives the tangent of θ. Taking the inverse gives θ, which can be used in the above formula to obtain d. One can also use trigonometric identities to express $\sin\theta$ in terms of $\tan\theta$. Yet another, but a simple approach is to use small angle approximation (provided the experimental apparatus is so designed that the n^{th} order fringe subtends a small angle at the source of diffraction), in which $\sin\theta \approx \tan\theta$, and hence one can replace $\sin\theta$ with the above-mentioned ratio.

Thus a can be determined, simply by measuring the distances between screen and wire and that between central maxima and n^{th} order fringe. This assumes beforehand that we know the wavelength of the light we are going to use.

6.3 Interference and measurement of Slit Width

Interference is yet another phenomenon giving rise to dark and bright fringes. Consider the case of double slit interference. If the slit width is negligible as compared to the slit separation we obtain sinusoidal intensity distribution giving rise to dark and bright fringes of equal width.

It is important to note a key difference and a similarity between single slit diffraction and double slit interference pattern. The separation between the dark fringes is uniform in both cases. The bright fringes, on the other hand, are uniform in case of interference but not so in the case of diffraction.

The fringe width (β) of the interference pattern is given by

$$\beta = \lambda \frac{D}{d}$$

where d is the slit separation and D is the separation between the slit and the screen. We can interpret the above result as the wavelength λ being magnified by the factor D/d.

In the experiment we determine D and d, hence we know the fringe width β, provided λ is known somehow.

6.4 Spring and it's analogy with a Diffraction Grating

A diffraction grating is an example of multiple slits, which contains a few thousand slits per cm. The intensity vs. position graph is interesting and useful to analyze. The single slit diffraction act as an envelope within which an interference pattern is observed. With an increase in the number of slits the peak becomes sharper and brighter. Secondary peaks of small intensity are observed in the dark region.

A spring, when viewed along a line perpendicular to the symmetry axis of spring, looks like two sets of parallel wires intersecting at an angle α. Each parallel set of wires is analogous to a diffraction grating.

Now the question is to identify what is it in the spring that is analogous to the slit in a diffraction grating. This question makes sense because of "**Babynet's principle**". It says that the diffraction pattern of a slit of width a is same as that of an opaque strip of width a. If a is the diameter of the wire used to make the spring and d is the distance between two consecutive wires in a given set of parallel wires, "Babynet's principle" makes it equivalent to consider both d and a as the slit width.

Invoking Heisenberg uncertainty principle, we conclude that smaller the dimension of the obstacle (uncertainty in position), more is the uncertainty in the momentum of photons, giving rise to fringes of larger width. So the diffraction pattern with a larger width corresponds to the width of the wire and the distance between two wires in a parallel set of wire corresponds to the fringe width of underlying interference pattern. Consider the following figure obtained in the lab.

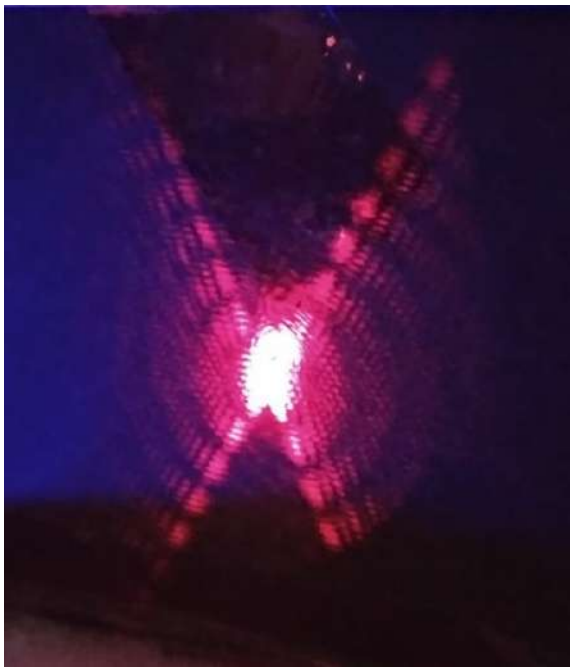

The "X" like structure is due to an angle between the two sets of parallel wires. With the angle between the two and inter-wire distance, we can determine the pitch of the spring as discussed in the following section.

6.5 Determination of the Pitch

6.5.1 Theory and Working Formula

A spring when viewed perpendicularly to its symmetry axis looks like two sets of parallel wires intersecting each other at an angle α. This is diagrammatically depicted in the following figure.

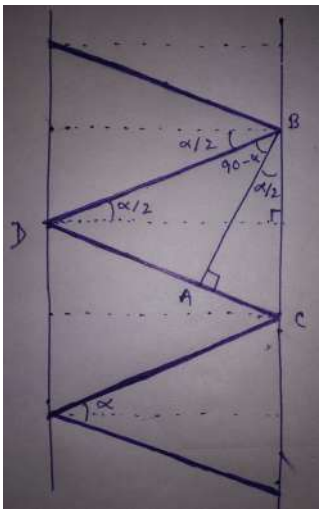

In this figure the pitch is $BC(= p$, say). The interference pattern obtained corresponds to the distance $AB(= d)$. The angle α is determined by the angle between two lines in the "X" like image obtained on the screen.

The fringe width of the interference pattern is given by

$$\beta = \lambda \frac{D}{d} \tag{9}$$

D is the distance between screen and the spring. β can be measured from the image obtained on the screen. Hence the inter-wire distance, d is given by

$$d = \lambda D/\beta \tag{10}$$

As shown in above figure, consider $\triangle ABC$. From simple trigonometry

$$BC = \frac{AB}{\cos(\alpha/2)}$$

Thus we have

$$p = \frac{\lambda D}{\beta \cos(\alpha/2)} \tag{11}$$

The above expression contains unknown variables all of which can be experimentally determined. Hence this is our working formula. We now describe the procedure we followed to determine these quantities.

6.6 Experimental method to determine required variables.

The wavelength of HeNe laser light was determined to be

$$\lambda = 619.31 \pm 14.58nm$$

We now describe how we determined other experimental parameters and the corresponding errors.

6.6.1 Determination of α and it's error.

To determine α we followed a method called *four point method*. Putting a blank white paper on the screen, we marked points far away from the center on the axes of the "X"-like image. It is better to take a few more points on an axis, though the method is named as four-point method. The name is justified because a minimum of four points, one on each axis is sufficient to determine the angle between them.

We took a few samples and determined the average to be

$$\alpha = 55.6^o$$

The frequency of data was 56^o. So we took α to be 56 degrees. The error in the angle was half the least count of the protractor, i.e. 0.5^o.

6.6.2 Determination of D and it's error

The value of D is determined by using the scale on the optical bench. The least count of the scale was 1 mm. Hence, the error in the measurement of D is half the least count i.e. 0.05 mm.

6.6.3 Determination of β and it's error

To determine β, we took blank paper sheets and placed it on the screen using a cello tape. We marked the dark lines of the interference pattern. From the spacing of pencil markings, different diffraction orders were distinguished. We used vernier calipers to measure the length of a few (3 to 5) interference fringes and then divided by the corresponding number in order to get the value of β. The least count of the vernier caliper used is 0.05 mm.

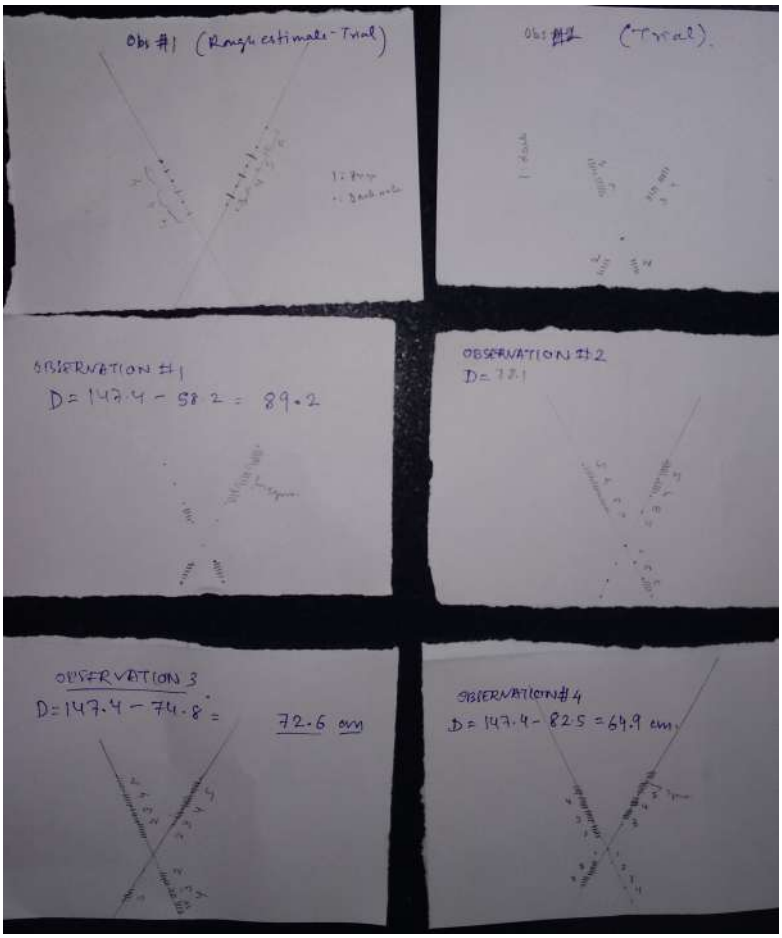

6.7 Analysis for Pitch determination

We took observations using the above method for four different values of D, and calculated pitch using the working formula. For each value of pitch, the error was propagated. The rounded average pitch and the mean square error was found to be

$$p = 0.066 \pm 0.002 \text{ cm} \tag{12}$$

The analysis was carried out in Libre Calc office software. The following pages show the analysis which led to the above result.

Determination of fringewidth

n is the number of fringes

α=56.0 degrees		0.977	radians
cos(α/2) =	0.882947593		
Wavelength =	619.31*10^(-7)		

Obs #	D	nβ	n	β	Pitch
	cm	mm	#	mm	cm
	89.2	3.8	4	0.950	0.065
	89.2	2.9	3	0.967	0.064
1	89.2	2.7	3	0.900	0.069
	89.2	3	3	1.000	0.062
	89.2	3.9	4	0.975	0.063
	89.2	3.65	4	0.913	0.068
	78.1	3.2	4	0.800	0.068
	78.1	2.55	3	0.850	0.064
2	78.1	2.6	3	0.867	0.062
	78.1	3.3	4	0.825	0.066
	78.1	3.1	4	0.775	0.070
	78.1	2.5	3	0.833	0.065
	72.6	2.45	3	0.817	0.062
	72.6	3.2	4	0.800	0.063
	72.6	1.5	2	0.750	0.067
	72.6	3	4	0.750	0.067
	72.6	3.1	4	0.775	0.065
3	72.6	1.6	2	0.800	0.063
	72.6	3.8	5	0.760	0.066
	72.6	2.9	4	0.725	0.069
	72.6	3.2	4	0.800	0.063
	72.6	2.2	3	0.733	0.069
	72.6	3	4	0.750	0.067
	64.9	1.9	3	0.633	0.071
	64.9	2.8	4	0.700	0.064
	64.9	2	3	0.667	0.067
	64.9	2.2	3	0.733	0.061
4	64.9	2	3	0.667	0.067
	64.9	2.7	4	0.675	0.067
	64.9	2.65	4	0.663	0.068
	64.9	2.85	4	0.713	0.063
	64.9	3.35	5	0.670	0.067
	64.9	2	3	0.667	0.067

Error Analysis

Propagated Errors in Pitch cm	square of error Cm^2
0.001759098	3.09442565E-06
0.001869422	3.49473864E-06
0.002060693	4.24645753E-06
0.001786448	3.19139756E-06
0.001703715	2.90264644E-06
0.001849441	3.42043311E-06
0.001915637	3.66966476E-06
0.00195394	3.81787999E-06
0.001901448	3.61550588E-06
0.00184068	3.3881013E-06
0.001997013	3.98806102E-06
0.00200934	4.03744583E-06
0.001922322	3.69532154E-06
0.001780804	3.17126382E-06
0.002738233	7.49791788E-06
0.001938842	3.75910896E-06
0.001856451	3.44641122E-06
0.002461586	6.05940471E-06
0.001789861	3.20360128E-06
0.00202889	4.11639291E-06
0.001780804	3.17126382E-06
0.00224774	5.05233616E-06
0.001938842	3.75910896E-06
0.002509697	6.29857894E-06
0.001902138	3.6181287E-06
0.002319068	5.37807851E-06
0.002009455	4.03790859E-06
0.002319068	5.37807851E-06
0.001999398	3.99759037E-06
0.002051802	4.20989012E-06
0.001856941	3.44823127E-06
0.001875527	3.51760108E-06
0.002319068	5.37807851E-06
RMS error:	0.002023056895

Physical Qty	Units	Numerical value
Average Pitch	cm	0.066
Error in pitch	cm	0.002

6.8 Dtermination of Diameter of the wire

As discussed earlier we are going to use the phenomena of diffraction to determine the diameter of the wire. We know the angular position of the dark diffraction fringes given by

$$a \sin\theta = n\lambda$$

If y_n is the position of n^{th} dark diffraction fringe with respect to the central maxima, the angle $\theta \approx y_n/D$. D is an experimentally measured quantity. Hence we have

$$y_n = n\frac{\lambda D}{a} \tag{13}$$

Since λ is known and D is measured, it is sufficient to plot y_n against n in order to determine a. The diameter of the wire a can be extracted from the slope of the plot.

In the experiment, we took data for four different values of D. For each of them straight line was fit for y_n vs n plot and from the slope, a was determined. The following plot shows y_n vs. n for each D.

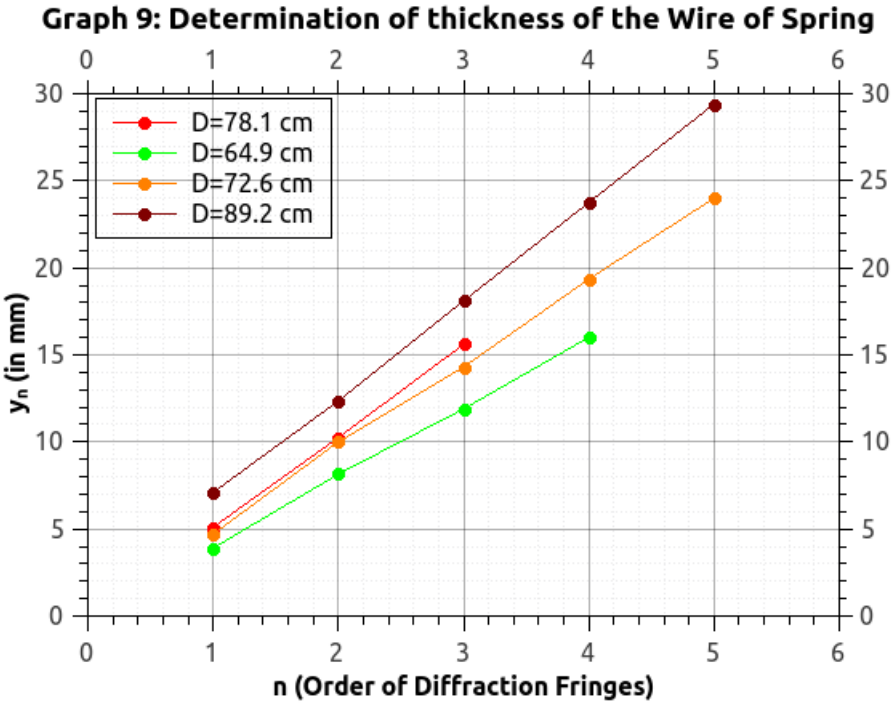

The following table shows the analysis of data obtained.

Measurement of The width of the spring's wire

D(cm)	n	y_n (in mm)	Slope	Error in slope	d(cm)	Error in d(cm)
	1	7.1				
	2	12.35				
89.2	3	18.1	5.6	0.05	0.00986	0.00025
	4	23.75				
	5	29.4				
	1	4.7				
	2	10				
72.6	3	14.3	4.79	0.08	0.00939	0.00027
	4	19.35				
	5	24				
	1	3.9				
64.9	2	8.15	4	0.06	0.01005	0.00028
	3	11.9				
	4	16				
	1	5.1				
78.1	2	10.25	5.25	0.06	0.00921	0.00024
	3	15.6				
					0.00963	0.00013

Average d	0.00963 cm
Mean square error	0.00013 cm

Hence, the diameter of the wire used to make the spring is $0.0963 \pm 0.0013 mm$.

6.9 Discussion

The pitch of the spring determined by using a traveling microscope was 0.066 ± 0.007 cm. This is in excellent agreement with the value of pitch we obtained using the laser diffraction method i.e., 0.066 ± 0.002 cm. Hence, the optical method is an effective way to determine the pitch of the spring. Also, the diameter of the wire used to make the spring is 0.00963 ± 0.00013 cm.

Having obtained the pitch and diameter of spring's wire, we are left with the determination of the helicity of spring to solve the structure of the spring completely. If the least count of the instrument measuring D is less than half the diameter of the spring then it is possible to determine the helicity. In that case, if we carefully measure the fringe widths then one of the axes of the image obtained will have comparatively smaller fringe widths. Hence we can determine which of the two sets of parallel wire is farther from the screen. Using this information the helicity can be easily determined. But we have not carried out this method because of unavailability of instruments of that precision. Also, it is not a useful method because we generally don't have such precise instruments. We should be able to devise some other methods to determine the helicity.

7 Further scope: Measuring the speed of Light

With the available apparatus, we see the possibility of being able to measure the speed of light.

We attempted to do so, using the beat frequencies of longitudinal modes of HeNe cavity. The reference for this experimental procedure is a 2010 paper by Daniel J. D'Orazio et. al. on "Measuring the speed of light using longitudinal modes in an open-cavity HeNe Laser" [4].

The laser beam emits over a range of frequencies given by the line shape function. In a cavity, depending on the length of it, only certain harmonics can exist. Thus due to a cavity, the line shape function becomes a comb-like plot with equidistant peaks. The nearest frequencies will superimpose to produce beats. One can measure these beat frequencies using RF spectrum analyzer. The frequency difference is a function cavity length. By measuring the change in cavity length and the corresponding change in the beat frequency, we can determine the speed of light.

While scanning over the range of frequencies, we obtained some peaks at kHz range. But later we realized that the source of these peaks was the electronics used in the power supplier of the laser.

8 Conclusion

We have determined the wavelength of the Helium-Neon laser to be 619.31 ± 14.58 nm, whereas the standard literature value is 632.8 nm. We studied the shape of the laser beam. It's properties matched with that of a Gaussian beam to a fair extent. The M^2 value was determined to be 0.751 ± 0.054. Qualitative analysis was done for the power dependence on resonator length, laser-cavity position and the discharge current. We made a small spring by wrapping a copper strand around the circuit wire, whose pitch was determined to be 0.066 ± 0.002 cm using the interference pattern obtained when the laser beam was illuminated on it. It matches well with traveling microscope measurement 0.066 ± 0.007 cm. The diameter of the wire was 0.0963 ± 0.0013 mm. We need more precision of instruments in order to measure the helicity of spring. Nevertheless, we can rely on the optical method to determine at least the two parameters mentioned above. Furthermore, one can devise methods to solve for double helix as an extension of this work. Also, the speed of light can be measured with the given apparatus, at least in principle. It remains only an experimental challenge, how to detect the beat frequency in the method described above using an RF spectrum analyzer.

Acknowledgements

I acknowledge the support of Lab assistants in the smooth conduct of the experiment. I express gratitude to Dr. Ritwick Das and Gunda Santosh Babu, whose suggestions helped us to proceed in some of the experimental steps. I am thankful for my labmate Pankaj Kumar, whose experimental expertise was crucial to do this experiment.

References

1. Ghatak, A. K., Thyagarajan, K. (1989). *Optical electronics*. Cambridge [England: Cambridge University Press.
2. PHYWE manual for Helium Neon laser, http://www.leermiddelen.be/en/getfile/0865693e_23121.pdf/bestand.html
3. Walker, J., Halliday, D., Resnick, R. (2011). *Fundamentals of physics*. Hoboken, NJ: Wiley.
4. D'Orazio et al.(2010), American Journal of Physics, 78, 524